Polymer 51 (2010) 1530–1539

Contents lists available at ScienceDirect

Polymer

journal homepage: www.elsevier.com/locate/polymer

Modeling the response of monofilament nylon cords with the nonlinear viscoelastic, simplified potential energy clock model☆

Douglas B. Adolf [a,*], Robert S. Chambers [b,1], Daniel C. Hammerand [b,2], Ming-Ya Tang [c,3], Kevin Westgate [c,4], Jim Gillick [c,5], Ihor Skrypnyk [d,6]

[a] Materials and Process Sciences Center Sandia National Laboratories, Albuquerque, NM 87185-0888, USA
[b] Engineering Sciences Center, Sandia National Laboratories, Albuquerque, NM 87185-0346, USA
[c] Global Materials Science, Goodyear Tire and Rubber Company, Akron, OH 44305, USA
[d] Tire-Vehicle Mechanics, Goodyear Tire and Rubber Company, Akron, OH 44305, USA

ARTICLE INFO

Article history:
Received 26 October 2009
Received in revised form
12 January 2010
Accepted 13 January 2010
Available online 25 January 2010

Keywords:
Nylon
Nonlinear viscoelasticity
Process history

ABSTRACT

The Simplified Potential Energy Clock Model has been previously shown to predict accurately glassy polymer responses such as yield, creep, enthalpy relaxation, and physical aging. It was now used to predict the behavior of monofilament Nylon fiber. Even though the fibers showed process-induced anisotropy, the simpler isotropic model could be used to describe uniaxial tests. The model predictions again accurately predicted a wide range of Nylon experimental data.

1. Introduction

While understanding the mechanical properties of Nylon fibers is helpful in the manufacture of fabrics, it gains greater importance in more demanding applications such as parachutes, seat belts, and sporting goods like tennis racquets and climbing ropes. When used as rubber reinforcement in tires, hoses, and conveyer belts, an understanding of the more general thermomechanical response becomes critical as cure temperatures and even operating temperatures exceed the glass transition temperature. Many of these applications employ cord rather than monofilament Nylon, but since the responses of the two are qualitatively similar, the monofilament fiber offers a simpler starting point to investigate intrinsic material behavior decoupled from the effects of cord structure.

One expects some type of viscoelastic model to predict fiber behavior since Nylon is a semi-crystalline thermoplastic. Yet the thermomechanical response is quite complicated, typically involving apparently negative coefficients of thermal expansion and irreversible effects, thus requiring an accurate and broadly applicable constitutive equation. The nonlinear viscoelastic, potential energy clock (PEC) model [1] and its simplified (SPEC) version [2] have been applied previously to several filled [3] and unfilled [4] thermosets and one thermoplastic, polycarbonate [5]. Accurate predictions were obtained for compressive and tensile yield at different temperatures, enthalpy relaxation, various physical aging tests, and creep. In this study, the response of a monofilament Nylon fiber to numerous tests were measured experimentally and predicted using the SPEC model.

While numerous studies have characterized fiber shrinkage and crystalline microstructure during heating [6–14], fewer have attempted to model the thermomechanical response of fibers [15–19], and the majority of these studies predict only room temperature response, thereby neglecting shrinkage and irreversibilities. Experimental studies clearly indicate the pronounced effect of

☆ Sandia is a multiprogram laboratory operated by Sandia Corporation, a Lockheed Martin Company, for the United States Department of Energy's National Nuclear Security Administration under contract DE-AC04-94AL85000.

* Corresponding author. Tel.: +1 (505) 844 4773; fax: +1 (505) 844 9624.
E-mail addresses: dbadolf@sandia.gov (D.B. Adolf), rschamb@sandia.gov (R.S. Chambers), dhammerand@m4-engineering.com (D.C. Hammerand), ming.ya.tang@goodyear.com (M.-Y. Tang), kwestgate@goodyear.com (K. Westgate), jim_gillick@goodyear.com (I. Gillick), ihor.skrypnyk@goodyear.com (I. Skrypnyk).
[1] Tel.: +1 (505) 844 0771; fax: +1 (505) 284 0135.
[2] Present address: Research Department, M4 Engineering, Long Beach, CA 90815, USA. Tel.: +1 (562) 981 7797; fax: +1 (562) 490 568.
[3] Tel.: +1 (330) 796 9015; fax: +1 (330) 796 7060.
[4] Tel.: +1 (330) 796 4277; fax: +1 (330) 796 3947.
[5] Tel.: +1 (330) 796 6403; fax: +1 (330) 796 3304.
[6] Tel.: +1 (330) 796 4509; fax: +1 (330) 796 3304.

0032-3861/$ – see front matter © 2010 Elsevier Ltd. All rights reserved.
doi:10.1016/j.polymer.2010.01.030

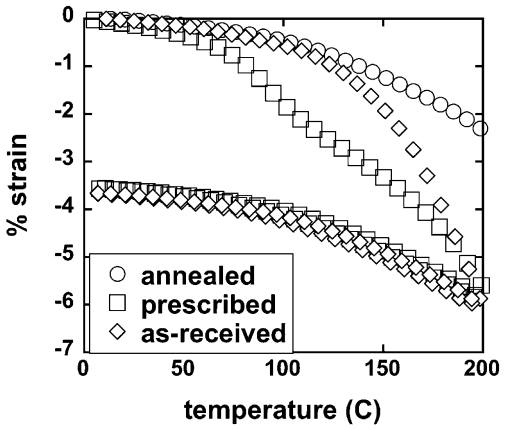

Fig. 1. A load of 2 N for the "processing history" of the "prescribed history" sample best matched the response of the "as-received" sample.

Table 1
Inputs to the isotropic SPEC model. Interpretation of the parameters when the model is applied to transversely isotropic Nylon fibers will be different.

Symbol	Isotropic physical interpretation
K_g	Glassy bulk modulus
K_∞	Equilibrium bulk modulus
G_g	Glassy shear modulus
G_∞	Equilibrium shear modulus
α_g	Glassy coefficient of thermal expansion
α_∞	Equilibrium coefficient of thermal expansion
C_1	1st WLF coefficient
C_2''	$C_2'' = C_2[1 + C_3\alpha_\infty]$ where C_2 is the 2nd WLF coefficient
C_3	A clock parameter producing a change in T_g with pressure and roughly equal to $(K\alpha)_d/(\rho_{ref}C_{Vd})$ where C_{Vd} is the viscoelastic decaying constant volume heat capacity, $(C_{Vg} - C_{V\infty})$
C_4	A clock parameter producing yield and roughly equal to $G_d/(\rho_{ref}C_{Vd})$
T_{ref}	Reference temperature (typically $T_g + 10\,^\circ$C)
ρ_{ref}	Reference density
f_s	Shear relaxation spectrum fit to the functional form in Eq. (11)
f_v	Bulk relaxation spectrum fit to the functional form in Eq. (11)

processing history on fiber response, yet the existing models ignore processing entirely. The present study differs from the literature studies in these two key features: a wide range of responses is investigated and predicted including complex thermal histories, and the processing history is explicitly included in the modeling.

2. Materials and experimental

The monofilament Nylon used in these studies had a roughly circular cross-sectional area with a diameter of 0.32 mm. All samples were stored in a desiccator containing Drierite for one week prior to testing since preliminary tests confirmed literature reports of large shifts in the glass transition temperature from moisture uptake. Transfer from the desiccator to the test chamber was accomplished as quickly as possible, and the heating chamber used nitrogen from a liquid dewar thus ensuring a dry testing environment.

Four types of tests were performed with a TA QMA-800 Dynamic Mechanical Analyzer (DMA).

(1) Ramp: stress controlled ramp (3 N/min) at 0 °C.
(2) Isostrain: constant strain (0, 1, 3, or 5%) held during a temperature profile of 0–200–0–200–0–200 °C (all ramps at 3 °C/min).
(3) Isoforce: constant load (0 or 8 N) held during a temperature profile of 0–200–0–200–0–200 °C (all ramps at 3 °C/min).
(4) Ratcheted isoforce: constant load (0 N) held during a temperature profile of 0–100–0–120–0–140–0–160–0–180–0–200 °C (all ramps at 3 °C/min).

All of these tests were performed on samples subjected to one of three histories.

(1) As-received: the monofilament is used directly off the manufacturer spool.
(2) Annealed: the manufacturer history is removed by heating under no load to 200 °C and back to 0 °C at 3 °C/min. Testing begins as the sample reaches 0 °C.
(3) Prescribed history: the sample is first annealed and then reheated to 200 °C at 3 °C/min where a 2 N load is applied. The sample is then cooled to 0 °C at 3 °C/min with the 2 N load applied. This load is removed at 0 °C, and the test begins.

These three histories allow us to probe the material free from processing effects (annealed), with a known "processing history" to examine its effect (prescribed), and with the actual processing history for comparison (as-received). For consistency between tests, the reference state (i.e., L_o) defining the engineering strain ($\Delta L/L_o$) was chosen to be the length immediately before the test started at 0 °C. The applied load of 2 N for the "processing history" of the "prescribed history" sample was chosen to match the free expansion (i.e., isoforce of 0 N) response of the "as-received" sample (Fig. 1)

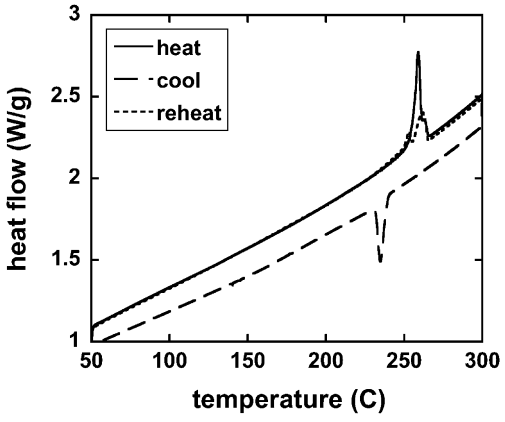

Fig. 2. DSC traces for determination of % crystallinity.

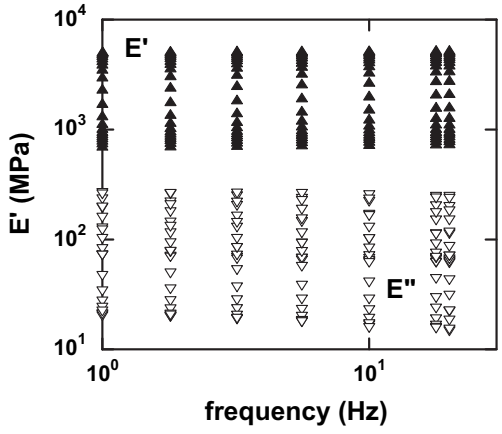

Fig. 3. Raw oscillatory tensile data for the annealed sample.

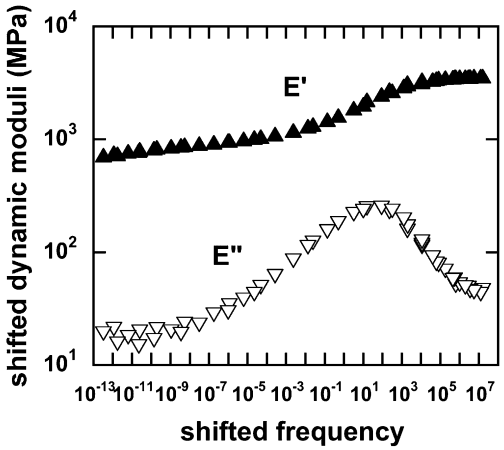

Fig. 4. Master curve for the annealed sample at a reference temperature of 100 °C.

over the temperature rang from 0 to 200 °C. This implies that the "as-received" cords experienced a constant force of roughly 2 N force as they cooled during processing temperatures to room temperature. This force was most likely not constant, and the thermal history was almost certainly different from the constant 3 °C/min cooling rate seen by the "prescribed history" samples, which accounts for the differences in the shapes of curves plotted in Fig. 1.

3. The simplified potential energy clock model for glassy polymers

3.1. Brief description of the model

The model derivation [1] follows the "Rational Mechanics" approach of Truesdell [20], which guarantees thermodynamic consistency by ensuring positive dissipation rates. The Helmholtz free energy, Ψ, is expanded in a Frechet series about the underlying equilibrated response, Ψ_∞, at the current state [21]. Small perturbations from equilibrium are expected so the series is truncated at second-order; the first-order terms vanish since the equilibrated free energy is a minimum. The equilibrated free energy is itself expanded in a Taylor series about a reference state conveniently chosen to be slightly above the nominal glass transition temperature.

The time derivative of the free energy can be used to define the Second Piola Kirchoff stress, $\underline{\underline{S}}$, entropy, η, and therefore all thermodynamic functions. The Laws of Thermodynamics state

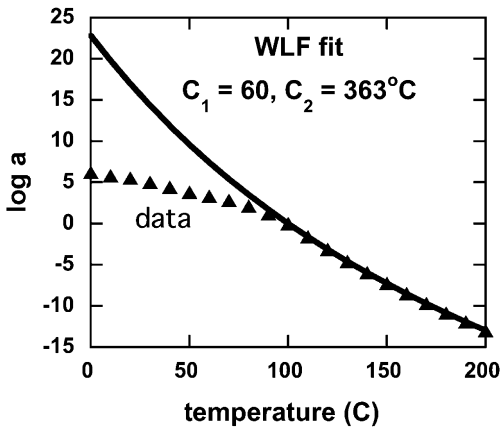

Fig. 5. The viscoelastic shift factor can be fit with the WLF equation.

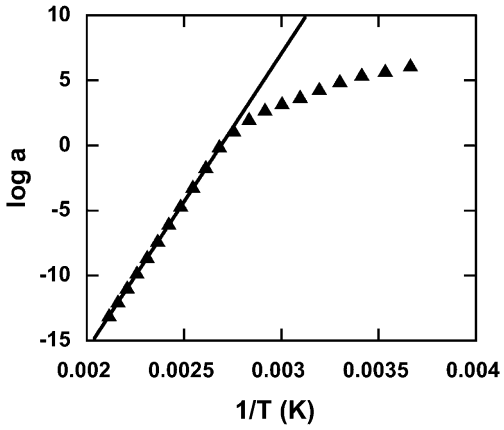

Fig. 6. The viscoelastic shift factor can be fit with an Arrhenius relationship.

$$\text{1st Law}: \frac{\mathrm{d}U}{\mathrm{d}t} = \frac{\mathrm{d}W}{\mathrm{d}t} + Q \text{ where } \frac{\mathrm{d}W}{\mathrm{d}t} = \frac{\underline{\underline{S}}}{\rho_{\mathrm{ref}}} : \frac{\mathrm{d}\underline{\underline{E}}}{\mathrm{d}t}$$

$$\text{2nd Law}: Q = T\frac{\mathrm{d}\eta}{\mathrm{d}t} - T\frac{\mathrm{d}\eta_{\mathrm{diss}}}{\mathrm{d}t}$$

$$\text{such that } \frac{\mathrm{d}\Psi}{\mathrm{d}t} = \left[\frac{\underline{\underline{S}}}{\rho_{\mathrm{ref}}} : \frac{\mathrm{d}\underline{\underline{E}}}{\mathrm{d}t}\right] - \left[\eta\frac{\mathrm{d}T}{\mathrm{d}t} + T\frac{\mathrm{d}\eta_{\mathrm{diss}}}{\mathrm{d}t}\right] \quad (1)$$

where $T\mathrm{d}\eta_{\mathrm{diss}}/\mathrm{d}t$ is the non-negative energy dissipation rate and $\underline{\underline{E}}$ is the Green-Lagrange strain measure defined as $1/2((\underline{\underline{F}}^T\underline{\underline{F}} - \underline{\underline{I}})$ with $\underline{\underline{F}}$ being the deformation gradient. Using the chain rule, the second Piola Kirchoff stress ($\underline{\underline{S}}$), entropy ($\eta$), and dissipation rate ($\mathrm{d}\eta_{\mathrm{diss}}/\mathrm{d}t$) are identified as partial derivatives of the free energy.

$$\frac{\mathrm{d}\Psi}{\mathrm{d}t} = \left(\frac{\partial\Psi}{\partial\underline{\underline{E}}}\right)_T : \frac{\mathrm{d}\underline{\underline{E}}}{\mathrm{d}t} + \left(\frac{\partial\Psi}{\partial T}\right)_{\underline{\underline{E}}}\frac{\mathrm{d}T}{\mathrm{d}t} + \left(\frac{\partial\Psi}{\partial t}\right)_{T,\underline{\underline{E}}} \text{ such that}$$

$$\underline{\underline{S}} = \rho_{\mathrm{ref}}\left(\frac{\partial\Psi}{\partial\underline{\underline{E}}}\right)_T,\ \eta = -\left(\frac{\partial\Psi}{\partial T}\right)_{\underline{\underline{E}}},\ \text{and } \frac{\mathrm{d}\eta_{\mathrm{diss}}}{\mathrm{d}t} = -\left(\frac{\partial\Psi}{\partial t}\right)_{T,\underline{\underline{E}}} \quad (2)$$

To accommodate a "material clock" that defines the dependence of viscoelastic relaxation rates on thermomechanical history [22,23], the Frechet series is expanded in "material time" intervals, $t^* - s^*$, rather than laboratory time intervals, $t - s$. The key feature, then, of any viscoelastic model is defining the material clock and the corresponding "viscoelastic shift factor", a. Here, the clock is a function of the potential energy, U^{pot}, of the system, which has been verified by molecular dynamics simulations [24,25].

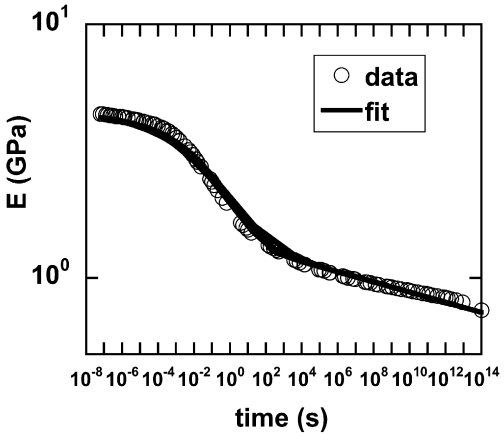

Fig. 7. Tensile relaxation modulus and fit using Eq. (11).

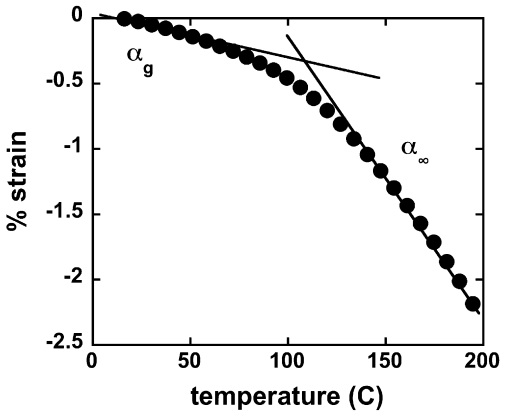

Fig. 8. Glassy and rubbery CTE's were extracted from the annealed isoforce test at 0 N.

$$\log a = -\frac{C_1\left(U^{\text{pot}} - U^{\text{pot}}_{\text{ref}}\right)}{C_2' + U^{\text{pot}} - U^{\text{pot}}_{\text{ref}}} \text{ and } t^* - s^* = \int_s^t \frac{\mathrm{d}x}{a(x)} \tag{3}$$

where C_1 and C_2' are related to the standard "WLF" coefficients [26].

$$\log a = -\frac{C_1\left(T - T_{\text{ref}}\right)}{C_2 + T - T_{\text{ref}}} \tag{4}$$

Note the similarity between Eqs. (3) and (4).

The total internal energy, U, can be calculated consistently from the Rational Mechanics framework. Since the potential energy is only part of the total, it is not directly available but can be approximated accurately [1]. The resulting expression is somewhat complicated and thus led to the SPEC model [2] in which several modest approximations were made. In the most useful of these, only a few dominant terms in the potential energy expression were retained leading to the following relationship.

$$\begin{aligned} U^{\text{pot}} = U^{\text{pot}}_{\text{ref}} &+ \beta_1 \left[\left\{ T - T_{\text{ref}} \right\} - \int_0^t \mathrm{d}s f_v(t^* - s^*) \frac{\mathrm{d}T}{\mathrm{d}s} \right] \\ &+ \beta_2 \left[\underline{\underline{\varepsilon}} - \int_0^t \mathrm{d}s f_v(t^* - s^*) \frac{\mathrm{d}\underline{\underline{\varepsilon}}}{\mathrm{d}s} \right] : \underline{\underline{I}} \\ &+ \beta_3 \int_0^t \int_0^t \mathrm{d}s\, \mathrm{d}u f_s(t^* - s^*, t^* - u^*) \frac{\mathrm{d}\underline{\underline{\varepsilon}}_{\text{dev}}}{\mathrm{d}s} : \frac{\mathrm{d}\underline{\underline{\varepsilon}}_{\text{dev}}}{\mathrm{d}u} \end{aligned} \tag{5}$$

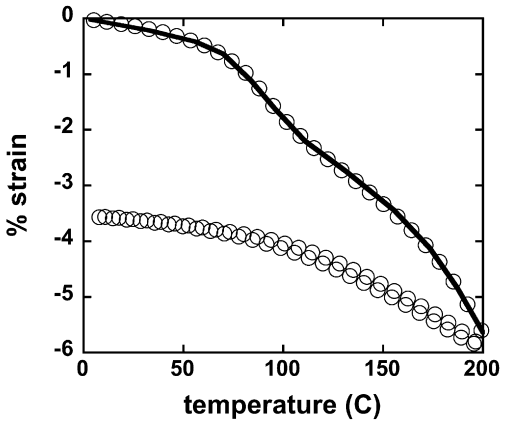

Fig. 9. The volumetric relaxation function was determined by fitting the first heating run (solid line) of the free expansion test (isoforce 0 N) for the "prescribed history" sample with known history.

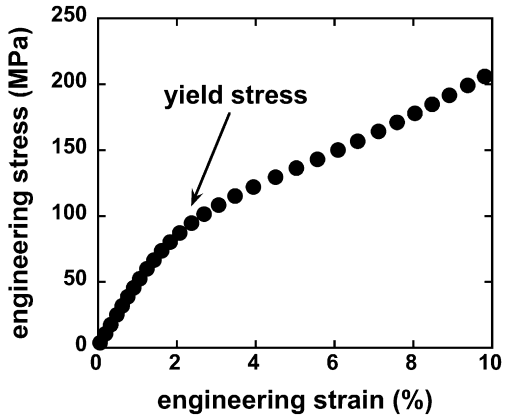

Fig. 10. The modest yield seen in the annealed ramp test was used to fix the parameter, C_4.

where the β_k are constants related to physically measurable quantities (heat capacity and bulk and shear moduli), f_v and f_s are the two independent relaxation functions. The Hencky strain measure was used in the PEC model, but was approximated in the SPEC model by the strain measure, $\underline{\underline{\varepsilon}}$, defined as the integral of the unrotated rate of deformation tensor, $\underline{\underline{d}}$ [27]. With this definition, the viscoelastic shift factor can be written as

$$\log a = -\frac{C_1 X}{C_2'' + X} \text{ where } C_2'' = C_2'/\beta_1 \text{ and}$$

$$\begin{aligned} X = &\left[\left\{ T - T_{\text{ref}} \right\} - \int_0^t \mathrm{d}s f_v(t^* - s^*) \frac{\mathrm{d}T}{\mathrm{d}s} \right] \\ &+ C_3 \left[\underline{\underline{\varepsilon}} - \int_0^t \mathrm{d}s f_v(t^* - s^*) \frac{\mathrm{d}\underline{\underline{\varepsilon}}}{\mathrm{d}s} \right] : \underline{\underline{I}} \\ &+ C_4 \int_0^t \int_0^t \mathrm{d}s\ \mathrm{d}u\ f_s(t^* - s^*, t^* - u^*) \frac{\mathrm{d}\underline{\underline{\varepsilon}}_{\text{dev}}}{\mathrm{d}s} : \frac{\mathrm{d}\underline{\underline{\varepsilon}}_{\text{dev}}}{\mathrm{d}u} \end{aligned} \tag{6}$$

Table 2
Values of the model parameters used for every prediction in this study.

Parameter	Value	Units
K_g	10.0	GPa
K_∞	5.0	GPa
G_g	2.5	GPa
$\mathrm{d}G_g/\mathrm{d}I_2$	30	GPa
G_∞	0	GPa
α_g	0	ppm/°C
α_∞	−800	ppm/°C
C_1	60	–
C_2''	363	°C
C_3	0	–
C_4	16000	–
T_{ref}	100	°C
ρ_{ref}	1176	kg/m^3
τ_1^s	0.1	seconds
τ_2^s	1.0	seconds
β_s	0.19	–
m_s	0.035	–
x_s	0.69	–
τ_1^v	10	seconds
τ_2^v	1.0	seconds
β_v	0.19	–
m_v	0.04	–
x_v	0.69	–

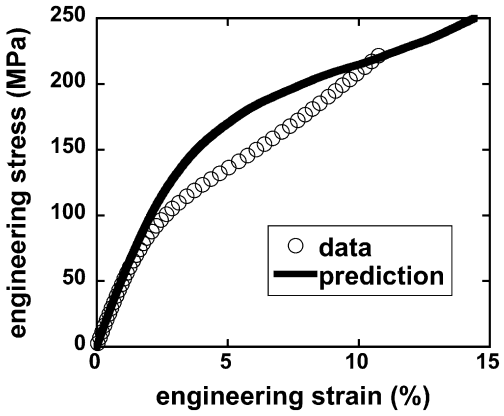

Fig. 11. Ramp data and predictions for the annealed sample.

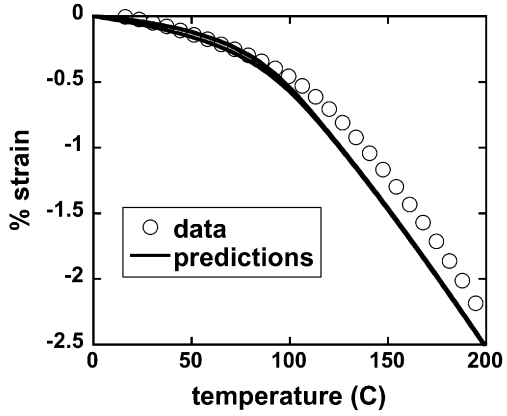

Fig. 13. Isoforce with 0 N load data and predictions for the annealed sample.

The material clock is embedded in the second Piola Kirchoff stress, $\underline{\underline{S}}$, derived from Eq. (2), and the resulting Cauchy stress, $\underline{\underline{\sigma}}$, is given by

$$\begin{aligned}\underline{\underline{\sigma}} &= \frac{\rho}{\rho_{\mathrm{ref}}}\underline{\underline{F}}\cdot\underline{\underline{S}}\cdot\underline{\underline{F}}^{T} = \frac{\rho}{\rho_{\mathrm{ref}}}\left[K_{\mathrm{d}}\int_0^t \mathrm{d}s f_v(t^*-s^*)\left(\frac{\mathrm{d}\underline{\underline{\varepsilon}}}{\mathrm{d}s}:\underline{\underline{I}}\right)\right.\\ &\left.-(K\alpha)_{\mathrm{d}}\int_0^t \mathrm{d}s f_v(t^*-s^*)\frac{\mathrm{d}T}{\mathrm{d}s}\right]\underline{\underline{I}}\\ &+\frac{2\rho G_{\mathrm{d}}}{\rho_{\mathrm{ref}}}\int_0^t \mathrm{d}s f_s(t^*-s^*)\left[\underline{\underline{R}}(t)\cdot\frac{\mathrm{d}\underline{\underline{\varepsilon}}_{\mathrm{dev}}}{\mathrm{d}s}(s)\cdot\underline{\underline{R}}(t)^{-1}\right]\\ &+\frac{\rho}{\rho_{\mathrm{ref}}}\left[K_{\infty 1}-K_{\infty}\alpha_{\infty}\left\{T-T_{\mathrm{ref}}\right\}\right]\underline{\underline{I}}\\ &+\frac{2\rho G_{\infty}}{\rho_{\mathrm{ref}}}\left[\underline{\underline{R}}\cdot\underline{\underline{\varepsilon}}_{\mathrm{dev}}\cdot\underline{\underline{R}}^{-1}\right] \end{aligned} \tag{7}$$

where K and G are the bulk and shear moduli, respectively, α is the volumetric coefficient of thermal expansion, ρ is the density, and $\underline{\underline{R}}$ is the rotational component from decomposition of the deformation tensor, $\underline{\underline{F}}$. The material parameters may depend on temperature as needed. The subscripts d and ∞ distinguish between the decaying viscoelastic and equilibrium values of a particular parameter. The decaying quantities are differences between the glassy and equilibrium bulk values; for example, K_{d} is equal to the difference between the glassy, K_{g}, and equilibrium, K_{∞}, bulk moduli. No degradation in predictive ability from adopting the approximations of the SPEC model has been observed [2].

3.2. Comparison with existing models for glassy polymers

Two frameworks have been proposed for describing the behavior of glassy polymers, plasticity and nonlinear viscoelasticity. While these two approaches may appear similar under certain situations, they have significant differences. Amorphous polymers are linear viscoelastic for infinitesimal strains, and no distinct change in the linear viscoelastic response is observed as rubbers are gradually cooled into the glass except that the relaxation times grow longer [24]. Nonlinear viscoelastic formalisms preserve this continuous transition between the rubbery and glassy states, and view mechanical yield as a natural consequence of the nonlinear relaxation behavior induced by loading. In contrast, plasticity theories by their very construction predict yield [28–30], but need to propose a second mechanism distinct from yield to describe the glass transition. Aside from the inherent problem of predicting a glass transition, plasticity theories also encounter difficulties explaining the concept of plastic flow in crosslinked materials that yield yet return to their original state when heated above the glass transition temperature. Consequently, one believes that the use of a single underlying, viscoelastic mechanism to describe both uncrosslinked and crosslinked polymers provides a more physically based constitutive description of glassy polymers.

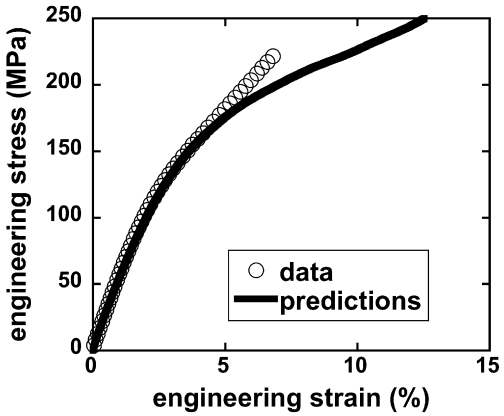

Fig. 12. Ramp data and predictions for the sample with prescribed history.

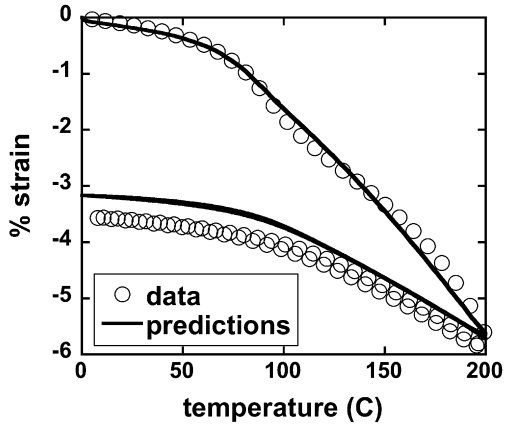

Fig. 14. Isoforce with 0 N load data and predictions for the prescribed history sample.

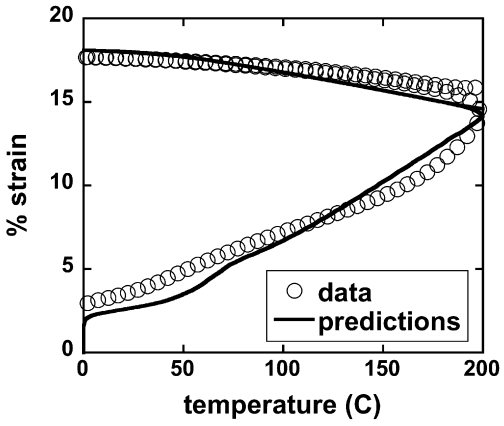

Fig. 15. Isoforce with 8 N load data and predictions for the annealed sample.

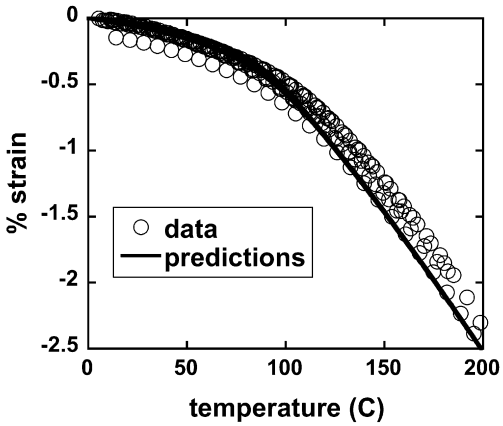

Fig. 17. Ratcheted isoforce data and predictions for the annealed sample.

A number of nonlinear viscoelastic constitutive equations have been developed for glassy polymers using the concept of a material clock to describe how relaxation rates depend on the state of the glass. For example, models using various definitions of free volume have predicted phenomena such as volume recovery, enthalpy relaxation, and physical aging with some success [31–34]. Mechanical yield in glassy polymers is a phenomenon of practical interest as well, and here quantitative predictions become more difficult. From a molecular view, the extremely slow relaxation rates of the glass are accelerated during the strain-ramp experiment. Stresses initially accumulate due to the ramp loading, but, at some point, relaxation rates are accelerated so much that stresses actually decrease viscoelastically; this point is the yield stress. While it is possible that a free volume approach could be used to explain yield in tension (due to the increase in volume from Poisson's ratio) or perhaps even in shear [35], it is not possible for this approach to predict yield in compression where free volume, as currently defined, decreases during the ramp forcing relaxation rates to likewise decrease. While free volume might explain many features of the dependence of polymer relaxations on external conditions, the inability of the current definition of free volume (i.e., packing fraction) to predict yield in all modes is a severe practical problem.

In another approach, the dependence of relaxation rates was attributed to "configurational entropy" [36], the entropy derived by considering only the potential energy of the system. This idea is also somewhat physically appealing in that viscoelastic relaxation rates slow as the avenues for cooperative motion become scarce as configurational entropy vanishes. In fact, free volume and configurational entropy-based constitutive equations perform similarly in many situations such as enthalpy relaxation [37]. Unfortunately, the difficulty again surfaces in predicting glassy mechanical yield. Both experimental data and elasticity theories suggest that entropy decreases with deformation in equilibrated rubbers [38], which would decelerate relaxation rates instead of producing the desired acceleration. Of course, entropy in glassy polymers may respond differently and might, in fact, increase during tensile tests due to a volume increase, thereby enabling tensile yield. Current configurational entropy models, however, are hard-pressed to predict an increase in configurational entropy during a compressive ramp, which is needed to accelerate relaxation rates and produce yield.

Attempts to predict compressive yield have incorporated additional dependences on a strain invariant [39] or the second stress invariant [40,41]. A stress clock has also been used in a more complicated viscoelastic model [42] that extended the phenomenological "fictive temperature" concept of Narayanaswamy [43]. It has been shown previously [1] that approaches employing the current strain predict qualitatively incorrect response under certain strain histories (load, hold, reload) and, therefore, cannot be employed in constitutive equations for predictions under arbitrary load histories. In particular, if a polymer is strained past yield, held at that strain until the stress relaxes, and then re-strained past yield, the second measured yield stress is similar to the first yield stress, contradicting the idea that total strain accelerates relaxation rates. Use of the stress invariant, however, is intriguing for prediction of nonlinear creep, but such models are inherently

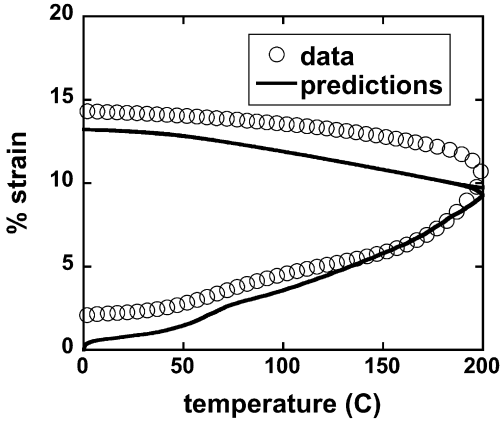

Fig. 16. Isoforce with 8 N load data and predictions for the prescribed history sample.

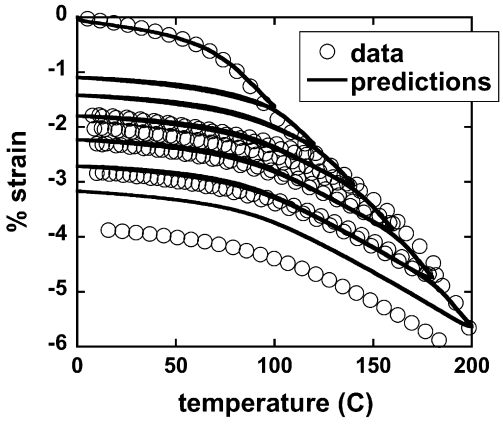

Fig. 18. Ratcheted isoforce data and predictions for the prescribed history sample.

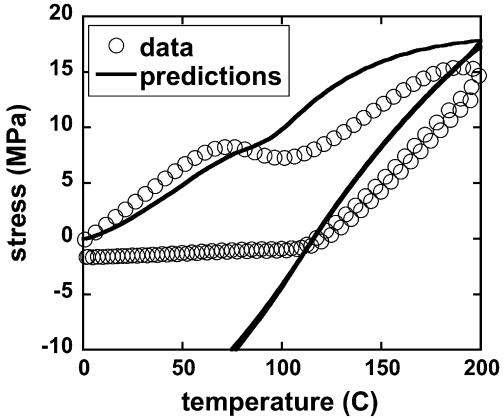

Fig. 19. Isostrain with 0% strain data and predictions for the annealed sample.

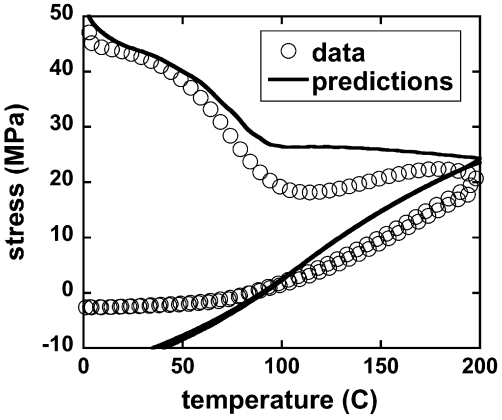

Fig. 21. Isostrain with 1% strain data and predictions for the annealed sample.

phenomenological and have not been extensively validated to assess comprehensive, quantitative, predictive capabilities for glassy polymer response such as yield. Some structural similarities between the potential energy and stress clock models have been discussed previously [1].

4. Application to Nylon

4.1. Crystallinity

Using differential scanning calorimetry (TA Q200) at 2 °C/min, the heat of melting of the as-received material (first heating run) is calculated to be 88 J/g (Fig. 2). If the heat of fusion of fully crystalline Nylon is taken to be 190 J/g [44], then the monofilament fibers used in these tests are roughly half crystalline. Note that the heat of melting from the second heating run is only 50 J/g so the thermal history does affect the percent crystallinity, and the thermal history during processing is significantly different from these lab tests.

Semi-crystalline polymers are rigorously two-phase materials so the Rational Mechanics approach used to develop the potential energy clock model would be technically inapplicable. However, our experience with filled polymers gives us hope that the approach may still yield accurate predictions. Even though the epoxies used previously were loaded up to 50 vol% with particulate fillers (glass, alumina, or microballoons) and therefore obviously two-phase systems, the predictions for various tests such as yield and enthalpy relaxation were still accurate [3].

If temperatures stay below the onset of the melting transition (roughly 200 °C), the crystalline domains could be viewed as effective cross-links, and the system would resemble an epoxy. Melting would be a complication, but the temperatures in the tests performed here never exceeded 200 °C. This restriction does not appear overly severe in real applications, since even tire cure temperatures would rarely exceed 200 °C. It is also possible that extremely large applied loads may disrupt the crystalline domains and "pull" chains out. This mechanism would not be captured by the potential energy clock model and would result in poor accuracy of the predictions.

4.2. Anisotropy

Nylon fibers are stretched considerably during their creation. This uniaxial stress is maintained as the crystallites form and then as the fiber vitrifies, thereby capturing orientation in both the crystalline and amorphous regions. While the fibers can attempt to erase the amorphous orientation as the temperature exceeds the glass transition, crystallite orientation persists until the domains have melted. Since the tests performed in this study remained below the melting transition, the crystalline orientation will always be present, and such intrinsic orientation may result in anisotropic fiber properties. Since the tests probed only the uniaxial response, the extent of such anisotropy is difficult to assess.

The potential energy clock model, as presented above, was developed for isotropic systems. It can and is being extended to orthotropic systems, but that level of complexity is unnecessary here since, again, only uniaxial response is considered. For an

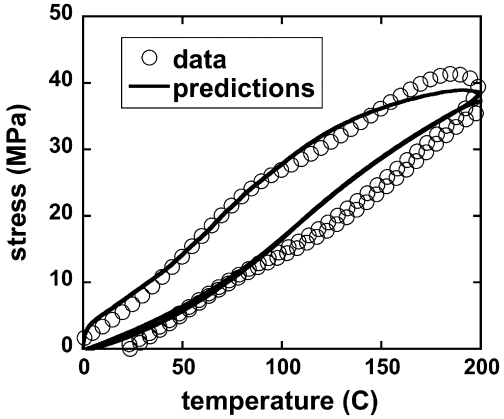

Fig. 20. Isostrain with 0% strain data and predictions for the prescribed history sample.

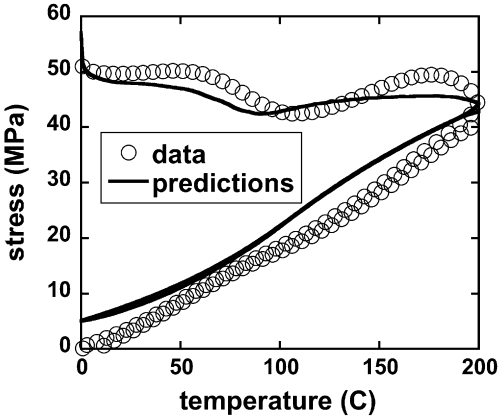

Fig. 22. Isostrain with 1% strain data and predictions for the prescribed history sample.

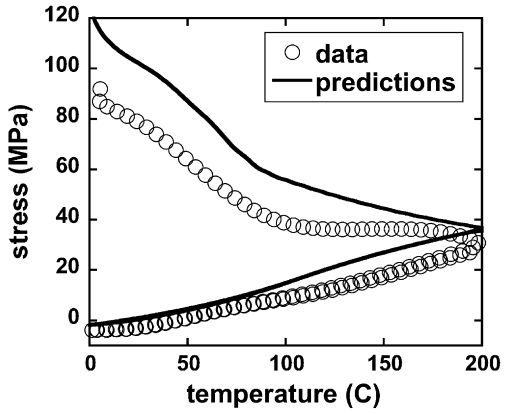

Fig. 23. Isostrain with 3% strain data and predictions for the annealed sample.

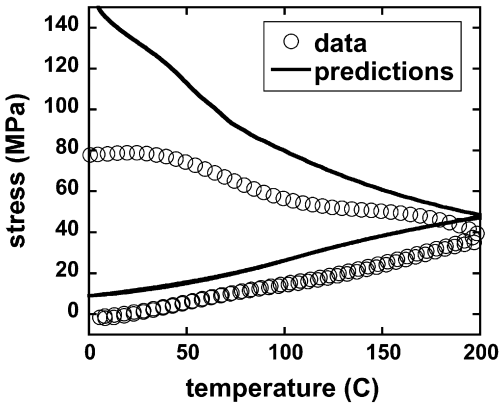

Fig. 25. Isostrain with 5% strain data and predictions for the annealed sample.

elastic, transversely isotropic material, the stresses along the primary fiber axes are given by

$$\begin{bmatrix}\sigma_{11}\\0\\0\end{bmatrix} = \begin{bmatrix}E_{11} & E_{12} & E_{12}\\ E_{12} & E_{22} & E_{23}\\ E_{12} & E_{23} & E_{22}\end{bmatrix}\begin{bmatrix}\varepsilon_{11}\\ \varepsilon_{22}\\ \varepsilon_{33}\end{bmatrix} - \begin{bmatrix}N_{11}\\ N_{22}\\ N_{22}\end{bmatrix}\Delta T \tag{8}$$

such that the uniaxial stress is given by

$$\sigma_{11} = E_{\text{eff}}\left(\varepsilon_{11} - \frac{\alpha_{\text{eff}}}{3}\Delta T\right) \text{ where } E_{\text{eff}} = E_{11} - \frac{2E_{12}^2}{E_{22}+E_{23}} \text{ and } \alpha_{\text{eff}} = \frac{3}{E_{\text{eff}}}\left(N_{11} - \frac{2E_{12}N_{22}}{E_{22}+E_{23}}\right) \tag{9}$$

Note that E in Eqs. (8) and (9) refers to a modulus and not the Green-Lagrange strain tensor; consistent yet conventional nomenclature is difficult. If only uniaxial response is examined, the structure of this equation for the orthotropic system is identical to the structure of the equation for the uniaxial stress in an isotropic system.

$$\sigma_{11} = E\left(\varepsilon_{11} - \frac{\alpha}{3}\Delta T\right) \text{ where } E = \frac{9KG}{3K+G} \tag{10}$$

Therefore, an inherently isotropic model, elastic or viscoelastic, can be used to mimic the response of an orthotropic material if predictions are limited to a subset of the possible behaviors. In this case, the Nylon fibers will be transversely isotropic, and tests will be restricted along the fiber axis. Of course, the isotropic model inputs must be re-interpreted in the light of a true, anisotropic material. For example, there is no true "bulk" modulus for an orthotropic material. More interestingly, the axial coefficient of thermal expansion for the orthotropic system may be negative while it must be non-negative for the isotropic system. Therefore, the magnitude and even sign of inputs to the isotropic model that mimics the anisotropic model may be unfamiliar. Table 1 lists the inputs to the isotropic, SPEC model.

5. Predictions

5.1. Model parameterization

Model parameters were determined by examining tests in a sequential fashion such that only a few constants were fit at a time. The tensile "master curve" was first determined on the annealed sample using the TA DMA in oscillatory mode with a strain amplitude of 1% over frequencies from 1 to 20 Hz and temperatures from 0 to 200 °C in 10 °C increments. The raw data are shown in Fig. 3, and the master curve is shown in Fig. 4.

The viscoelastic shift factor used to construct the master curve at a reference temperature of 100 °C is shown in Fig. 5 and could be fit with the WLF equation in the equilibrated state above the glass transition, albeit with unusual parameters. Surprisingly, the shift factor for this equilibrated, anisotropic material could be described just as well by an Arrhenius relationship (Fig. 6).

The master curve was transformed into the time domain to produce the tensile relaxation modulus (Fig. 7), which was then fit with the following phenomenological function form.

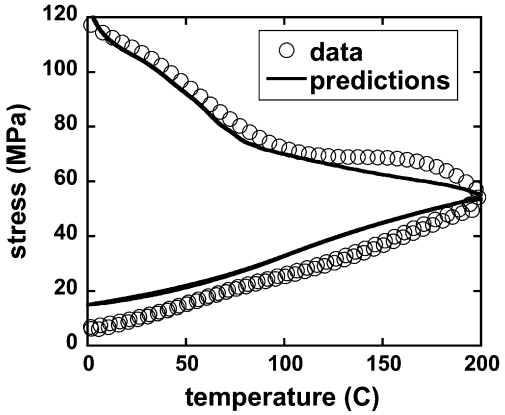

Fig. 24. Isostrain with 3% strain data and predictions for the prescribed history sample.

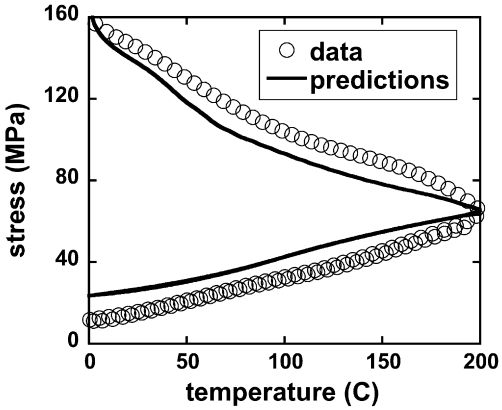

Fig. 26. Isostrain with 5% strain data and predictions for the annealed sample.

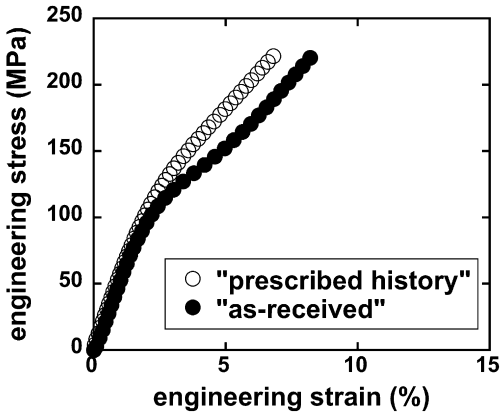

Fig. 27. Ramp data for the prescribed history and as-received samples.

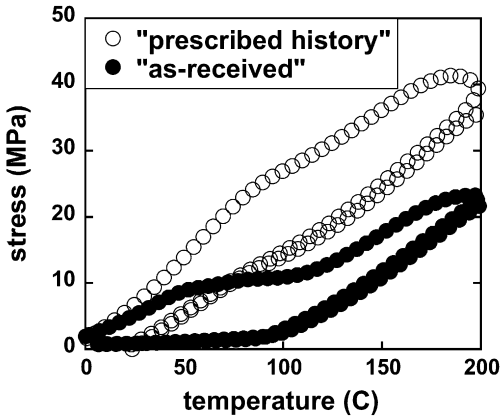

Fig. 29. 0% isostrain data for the prescribed history and as-received samples.

$$E(t) = (E_g - E_\infty)\left[x_s e^{-(t/\tau_1^s)^{\beta_s}} + \frac{(1-x_s)}{(1+t/\tau_2^s)^{m_s}}\right] + E_\infty = (E_g - E_\infty) f_s(t) + E_\infty \quad (11)$$

This function form allows a relatively steep decay from the glassy modulus (using the stretched exponential) and a lethargic decay at longer time (the power law) as seen in Fig. 7. Typical values for the glassy and rubbery bulk moduli were assumed (5 and 3 GPa, respectively), and the glassy and shear moduli were chosen to fit the tensile response. Subsequent analysis demonstrated little sensitivity of any prediction to the exact value of the bulk moduli around these initial choices.

The coefficients of thermal expansion far from the glass transition were assumed constant (no temperature dependence) and extracted directly from the free expansion tests (isoforce at 0 N) on the annealed sample (Fig. 8).

Notice that these effective CTE's are negative, which is allowed for an anisotropic material.

The normalized volumetric relaxation function was fit using the same form as in Eq. (11),

$$f_v(t) = \left[x_v e^{-(t/\tau_1^v)^{\beta_v}} + \frac{(1-x_v)}{(1+t/\tau_2^v)^{m_v}}\right] \quad (12)$$

which again required five fitting parameters: τ_1^v, τ_2^v, β_v, m_v, and x_v. These were initially set equal to the corresponding tensile relaxation function and then modified slightly to reproduce the first heating run (solid line) of the free expansion test (isoforce 0 N) for the "prescribed history" sample with known history (Fig. 9).

The clock parameter, C_4, is the term responsible for producing yield predictions. It was determined by fitting the ramp test on the annealed sample (Fig. 10).

The final parameter, C_3, was set equal to zero, and variations upon this did not improve any predictions for the tests performed here.

The resulting parameters are shown in Table 2 and were used consistently without adjustment on every prediction in this study.

5.2. Model predictions

Across the board, the model predictions are in good agreement with all test data for both the annealed and prescribed history samples (Figs. 11–26). Note that in the isostrain tests, the predicted stresses can become negative whereas the actual fibers buckle in compression and can never produce negative stresses. The real but minor differences that do appear between predictions and data should not cloud the conclusion that the complex response of these anisotropic fibers over a wide range of tests is captured with only a viscoelastic model employing a potential energy "material clock". Also not to be missed is the fact that the disparity between the first and subsequent heating runs in the isoforce and isostrain tests is not primarily due to intricate crystalline transitions or temperature

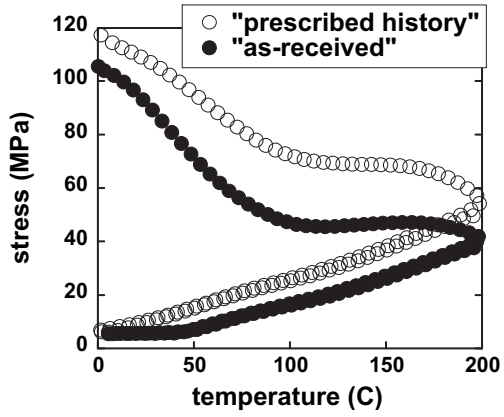

Fig. 28. Isoforce data for the prescribed history and as-received samples.

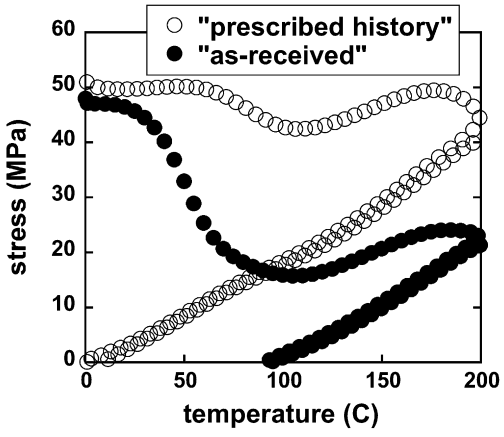

Fig. 30. 1% isostrain data for the prescribed history and as-received samples.

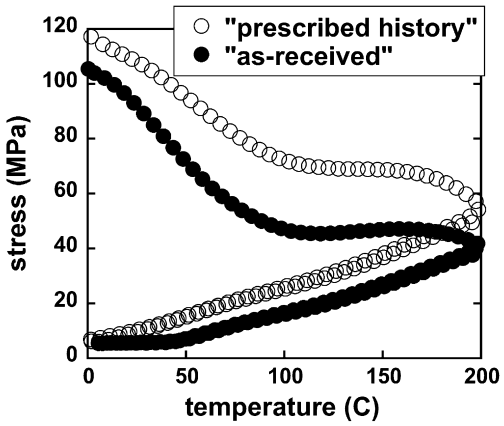

Fig. 31. 3% isostrain data for the prescribed history and as-received samples.

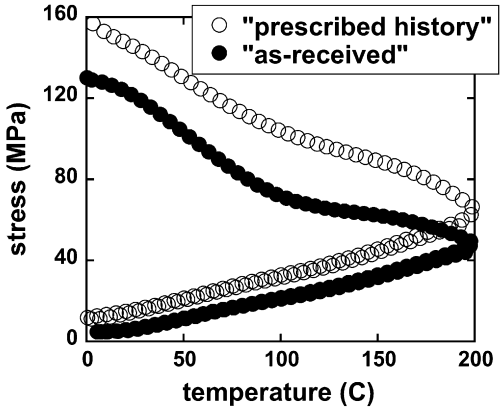

Fig. 32. 5% isostrain data for the prescribed history and as-received samples.

dependent hydrogen bonding mechanisms[45,46] but can be attributed simply to viscoelastic decay of the processing history.

If the "processing history" is known as it was for the samples with a prescribed history, the model appears to predict response quite well. It may be asked, however, if the behavior of the as-received samples is similar to these or qualitatively different. The free expansion responses were shown previously in Fig. 1 to be quite similar when an applied load of 2 N for the prescribed history was chosen to mimic the as-received samples in this test. Further comparisons between the prescribed history and as-received samples are shown in Figs. 27–32. While some differences are seen in the isostrain tests with 0 and 1% applied strain, the ramp, isoforce, and isostrain tests with larger applied strains are very similar. Some differences between these samples are expected since the histories are not identical. Therefore, the model should predict the responses of the as-received samples with equal fidelity if the histories were available.

6. Conclusions

The simplified potential energy clock model (SPEC) accurately predicts a wealth of nonlinear viscoelastic behavior. With this tool, it is now possible to predict the response of complex materials such as Nylon, an anisotropic fiber processed under high stresses and strains. If the preponderance of predictions match data, it implies that the complicated experimental behavior arises from nonlinear viscoelasticity. That is, the model can be used to understand the underlying mechanisms of thermophysical response. Similar exercises are being performed on biaxially stretched polyethylene films used for capacitor dielectrics.

Not to be minimized is the ability to use this new predictive capability to predict the evolution of properties over time in components employing Nylon fibers and the thermal response of Nylon cords used as rubber reinforcement. In addition, it may be possible to "reverse engineer" the processing history of an incoming fiber, which could illuminate possible in-house processing strategies to optimize fiber response.

References

[1] Caruthers JM, Adolf DB, Chambers RS, Shrikhande P. Polymer 2004;45:4577.
[2] Adolf DB, Chambers RS, Neidigk Matthew A. Polymer 2009;50:4257.
[3] Adolf DB, Chambers RS. J Polym Sci B Polym Phys 2005;43:3135.
[4] Adolf DB, Chambers RS, Flemming J. J Rheol 2007;51:517.
[5] Adolf DB, Chambers RS, Caruthers JM. Polymer 2004;45:4599.
[6] Grebowicz JS, Brown H, Chuah H, Olvera JM, Wasiak A, Sajkiewicz P, et al. Polymer 2001;42:7153.
[7] Huisman R, Heuvel HM. J Appl Polym Sci 1989;37:595.
[8] Aou K, Shuhui K, Shaw LH. Macromolecules 2005;38:7730.
[9] Fu Y, Annis B, Boller A, Jin Y, Wunderlich B. J Polym Sci B Polym Phys 1994;32:2289.
[10] Lim JY, Kin SY. J Polym Sci B Polym Phys 2001;39:964.
[11] Simal AL, Martin AR. J Appl Polym Sci 1998;68:441.
[12] Heuvel HM, Lucas LJ, van den Heuvel CJM, de Weijer AP. J Appl Polym Sci 1992;45:1649.
[13] Govaert LE, Lemstra P. J Colloid Polym Sci 1992;270:455.
[14] Wu Z, Zhang A, Shen D, Leland M, Harris FW, Cheng SZD. J Therm Anal 1996;46:719.
[15] Chailleux E, Davies P. Mech Time-Dependent Mat 2005;9:147.
[16] Drozdov AD, Kalamkarov AL. Polym Eng Sci 1996;36:1907.
[17] Blanc RH, Ravasoo A. Mech Mater 1996;22:301.
[18] Baltussen JJM, Northolt MG. Polymer 2004;45:1717.
[19] Wortmann F-J, Schulz KV. Polymer 1994;35:2108.
[20] Trusdell CA, Noll W. Handbuch der Physik, III/3. In: Flugge S, editor. , New York: Springer Verlag; 1965. Rational Thermodynamics, New York: Springer-Verlag, 1984 (Lectures 1 and 2).
[21] Coleman BD. Arch Rat Mech 1964;17:1.
[22] Hopkins IM. J Polym Sci 1958;28:631.
[23] Moreland LW, Lee EH. Trans Soc Rheol 1960;4:233.
[24] Budzein J, McCoy JD, Adolf DB. J Chem Phys 2004;121:10291.
[25] Heffernan JV, Budzein J, Wilson AT, Baca RJ, Aston VJ, Avila F, et al. J Chem Phys 2007;126:184904.
[26] Ferry JD. Viscoelastic properties of polymers. , New York: Wiley; 1980.
[27] Flanagan DP, Taylor LM. Comp Methods Appl Mech Eng 1987;62:305.
[28] Boyce MC, Parks DM, Argon AS. Mech Mater 1988;7:15.
[29] Arruda EM, Boyce MC. Int J Plast 1993;9:697.
[30] G'Sell C, Jonas JJ. J Mater Sci 1981;16:1956.
[31] Hutchinson JM, Kovacs AJ. J Polym Sci B Polym Phys 1976;14:1575.
[32] Chow TS. Macromolecules 1984;17:2336.
[33] Robertson RE, Simha R, Curro JG. Macromolecules 1984;27:911.
[34] Drozdov AD. Polymer 1998;39:1327.
[35] Wang TT, Matsuoka S. J Polym Sci B Polym Phys 1980;18:586.
[36] Adam G, Gibbs JH. J Chem Phys 1965;43:129.
[37] Hodge IM. J Non-Cryst Solids 1994;169:211.
[38] Flory PJ. Principles of polymer chemistry. Ithaca: Cornell University Press; 1953.
[39] Knauss WG, Emri I. Polym Eng Sci 1987;27:86.
[40] Schapery RA. Polym Eng Sci 1969;9:295.
[41] Popelar CF, Lechti KM. Mech Time-Dependent Mat 2003;7:89.
[42] Grassia L, D'Amore A. Phys Rev E 2006;74:021504-1.
[43] Narayanaswamy O. J Am Ceram Soc 1988;71:900.
[44] Starkweather HW, Zoller P, Jones GA. J Polym Sci B Polym Phys 1984;22:1615.
[45] Jones NA, Cooper SJ, Atkins EDT, Hill MJ, Franco L. J Polym Sci B Polym Phys 1997;35:675.
[46] Murthy NS. J Polym Sci B Polym Phys 2006;44:1763.